Articles

Simple Route to Bis(3-indenyl)methanes and the Synthesis, Characterization, and Polymerization Performance of Selected *racemic*-Dichloro[methylenebis(R_n-1-indenyl)]-zirconium Complexes

Vu Anh Dang,[‡] Lin-Chen Yu,[‡] Davide Balboni,[§] Tiziano Dall'Occo,[§] Luigi Resconi,*[,§] Pierluigi Mercandelli,[#] Massimo Moret,[#] and Angelo Sironi[#]

Montell Polyolefins, Research & Development Center, 912 Appleton Road, Elkton, Maryland 21921, Centro Ricerche G. Natta, P.le G. Donegani 12, 44100 Ferrara, Italy, and Dipartimento di Chimica Strutturale e Stereochimica Inorganica, Università di Milano, Via Venezian 21, 20133 Milano, Italy

Received March 25, 1999

A large range of bis(R_n-3-indenyl)methanes were obtained in good to fair yields with the base-catalyzed condensation between formaldehyde and (substituted) indenes. For example, bis(indenyl)methane and bis(4,7-dimethylindenyl)methane have been synthesized in 70% and 50% yield, respectively, from the corresponding indenes. Typical reaction conditions are as follows: indene in DMF or DMSO, 0.5 equiv of CH_2O, 0.2−0.5 equiv of EtONa, room temperature. This process provides an inexpensive and atom-efficient protocol for the synthesis of methylene-bridged ligands, providing a facile entry into methylene-bridged *ansa*-zirconocenes: MAO-activated C_2-symmetric *rac*-dichloro[methylenebis(η^5-1-indenyl)]zirconium (**1**) and *rac*-dichloro[methylenebis(4,7-dimethyl-η^5-1-indenyl)]zirconium (**2**) polymerize ethylene to low molecular weight, vinyl-terminated linear polyethylene, and liquid propylene to low molecular weight, low isotacticity polypropylene. The microstructure, molecular weight, and end-group structure of these isotactic polypropylenes (*i*-PP) are compared to those from *rac*-[isopropylidenebis(1-indenyl)]$ZrCl_2$ (**3**), *rac*-[ethylenebis(1-indenyl)]$ZrCl_2$ (**4**), *rac*-[ethylenebis(4,7-dimethyl-1-indenyl)]$ZrCl_2$ (**5**), and the silicon-bridged *rac*-[dimethylsilylbis(1-indenyl)]$ZrCl_2$ (**6**). The molecular structures of **1** and **2** have been determined and compared to those of **3**−**6**. In liquid monomer at 50 °C, the amount of secondary insertions increases on going from the more open to the more hindered systems. At the same time, there is an increase of the fraction of secondary units undergoing isomerization from the normal 2,1 unit to the 3,1 unit (tetramethylene sequence).

Introduction

ansa-Metallocene ligands with a single carbon bridge have been obtained via reaction of cyclopentadienyl or indenyl anions with CH_2Br_2 or CH_2I_2[1] or by reaction of a fulvene (or benzofulvene) with cyclopentadienyl, indenyl, or fluorenyl anions.[2] In the case of bisindenyl ligands, the above reactions are scarcely efficient. Recently, Nifant'ev and co-workers,[3] and later Jensen,[4] disclosed a simple, one-pot procedure for the syntheses of bis(cyclopentadienyl)propane and bis(indenyl)propane. The simplest case is the condensation of indene and acetone in DME, which gives 2,2-bis(3-indenyl)-propane in up to 70% yield:[3]

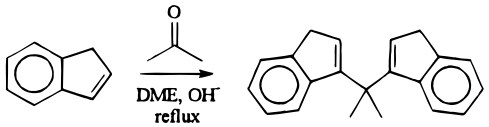

This reaction is highly convenient, since all reagents are inexpensive, it does not require air- and moisture-free conditions, and it is atom-efficient,[5] since in principle the only byproduct is water. It can however lead to formation of bridged benzofulvenes, which are dif-

[‡] Montell Polyolefins.
[§] Centro Ricerche G. Natta.
[#] Università di Milano.

(1) (a) Schaltegger, H.; Neuenschwander, M.; Meuche, D. *Helv. Chim. Acta* **1965**, *48*, 955. (b) Ewen, J.; Elder, M.; Jones, R.; Haspeslagh, L.; Atwood, J.; Bott, S.; Robinson, K. *Makromol. Chem., Macromol. Symp.* **1991**, *48/49*, 253.

(2) See for example ref 1b, and: Hafner, K.; Thiele, G. *Tetrahedron Lett.* **1984**, *25*, 1445. Green, M. L. H.; Ishihara, N. *J. Chem. Soc., Dalton Trans.* **1994**, 657.

(3) Nifant'ev, I. E.; Butakov, K. A.; Aliev, Z. G.; Urazowski, I. F. *Metalloorg. Khim.* **1991**, *4*, 1265. Nifant'ev, I. E.; Ivchenko, P. V.; Borzov, M. V. *J. Chem. Res., Synop.* **1992**, 162. Nifant'ev, I. E.; Borzov, M. V.; Ivchenko, P. V.; Yarnikh, V. L.; Ustynyuk, Yu. A. *Organometallics* **1992**, *11*, 3462. Nifant'ev, I. E.; Ivchenko, P. V.; Kuz'mina, L. G.; Luzikov, Yu. N.; Sitnikov, A. A.; Sizan, O. E. *Synthesis* **1997**, 469.

(4) Yang, Q.; Shuguang, S.; Hoffman, M. R.; Jensen, M. D. 212th ACS National Meeting, 1996, ORGN 008.

(5) Rouhi, A. M. *Chem. Eng. News* **1995**, *June 19*, 32.

10.1021/om990211g CCC: $18.00
Publication on Web 08/18/1999

Table 1. Synthesis of Bis(indenyl)methanes

indenyl derivative	CH_2O	solvent/base	temp (°C)/time (h)	yield (%)
indene	formalin	DMF/NaOEt	25/12	70
4,7-dimethylindene	formalin	DMF/NaOEt	25/12; 80/4	48
4,7-dimethylindene	formalin	DMSO/NaOEt	25/12; 80/4	50
4,7-dimethylindene	paraformaldehyde	DMSO/NaOEt	25/12; 65/8	33
4,7-dimethylindene	paraformaldehyde	DME/NaOEt	25/12	0
3-phenyl-4,6-dimethylindene	formalin	DMF/NaOEt	25/12	79
3-*tert*-butylindene	paraformaldehyde	DMSO/*t*-BuOK	25/12	82
fluorene	paraformaldehyde	DMF/NaOEt	25/12	34

ficult to remove from the reaction mixture, and in addition is limited to indenes without substituents in the 7 position. This reaction, in fact, cannot be applied to 4,7-dimethylindene, even under more severe conditions (DMSO/*t*-BuOK, 110 °C, 10 h). To overcome these limitations, we have sought the synthesis of *methylene*-bridged bis(substituted)indenyl ligands using formaldehyde, with the aim to expand the range of achievable ligands for chiral zirconocene catalysts and to make them simpler. Our first attempt, using DME as a solvent, was unsuccessful.

We report here the synthesis of methylene-bridged bisindenyl ligands via the base-catalyzed condensation of indenes with formaldehyde in more polar solvents, which in turn allows a facile entry to a large variety of C_2-symmetric, isospecific zirconocenes.[6] This new method is more convenient than those via fulvene or CH_2X_2 and a recently published method that uses chloromethylpivalate.[7]

Results and Discussion

Synthesis of the Ligands. The base-catalyzed condensation between formaldehyde and (substituted) indenes is a new, simple, inexpensive, and atom-efficient protocol for the synthesis of a wide variety of bis(substituted)indenylmethanes, providing a facile entry into methylene-bridged *ansa*-zirconocenes. For example, bis(indenyl)methane and bis(4,7-dimethylindenyl)methane have been synthesized in 70% and 50% yield, respectively, from the corresponding indenes in DMF or DMSO as solvents (Table 1). The reaction is catalyzed by bases such as KOH, NaOH, *t*-BuOK, or EtONa, with base/indene ratios as low as 0.2. In some cases, the temperature of the reaction must be kept below 50 °C to avoid isomerization to the conjugated 1-(3-indenylvinylidenyl)indane.

As is the case for Nifant'ev's acetone/indene condensation, the appeal of using formaldehyde rather than other bridging moieties is multifold: the main advantages are that moisture- and air-free procedures are no longer required and the higher atom-efficiency of the process. In addition, we discovered that the base can be catalytic, that benzofulvene byproducts are not observed in the final product, and that neither the indenes nor the solvents need distillation before use. The downside is the sometimes unavoidable formation of higher condensation products and the lower than quantitative yields obtained in practice. All things considered, comparing bisindenyl ligands with different bridges, the present process is more convenient when cheap indenes are used. If the methylene-bridged ligands are the target, then the present process is the most convenient presently available. The formaldehyde can be either in polymeric form or in aqueous solution. Various conditions for the synthesis of bis(4,7-dimethyl-3-indenyl)methane are shown in Table 1. The results

Table 2. Condensation of 3-Phenyl-4,6-dimethyl-1-indene with Formaldehyde and Acetone

aldehyde or ketone	solvent/base	temp (°C)/time (h)	yield (%)
formalin	DMF/NaOEt	25/12	79
formalin	DMF/KOH	25/12	58
paraformaldehyde	DMF/NaOEt	25/12	54
formalin	DME/KOH	25/12	traces
formalin	DMF/NaOEt	80/6	65
acetone	DME/KOH	80/48	63

indicate that a strong base in a highly polar aprotic solvent is preferred for the preparation of bis(4,7-dimethyl-3-indenyl)methane:

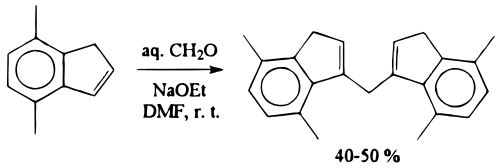

This methodology is also applicable to highly substituted indenes, allowing the synthesis of sterically crowded ligands, such as bis(fluorenyl)methane: the reaction of fluorene and paraformaldehyde in the presence of a base in dimethyl sulfoxide afforded bis(fluorenyl)methane in 34% yield (eq 1). A two-step procedure (eq 2) through dibenzofulvene (**7**) yielded

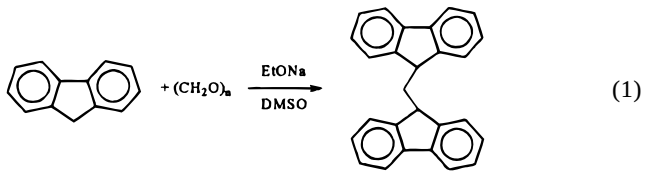

(1)

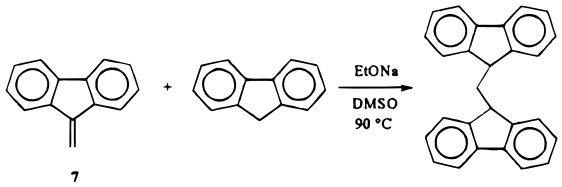

(2)

similar results. This demonstrates the efficiency of this one-pot procedure. The reaction of 3-*tert*-butylindene with paraformaldehyde in DMSO/*t*-BuOK yielded bis(1-*tert*-butyl-3-indenyl)methane in 82% yield. The reaction of formaldehyde with 3-phenyl-4,6-dimethylindene, using different bases and solvents, yielded bis(1-phenyl-5,7-dimethyl-3-indenyl)methane in good yields (Table 2). Since the proton of this indene is more acidic than that of 4,7-dimethylindene, yields for these reactions were higher as compared to 4,7-dimethylindene. Again, the

(6) After this work was finished, a similar process for the synthesis of methylene-bridged ligands was described in the patent literature: Küber, F.; Riedel, M.; Schiemenz, B. Eur. Pat. Appl. 832,866 A2 to Targor, 1998.

reaction with a strong base and a polar aprotic solvent afforded the highest yield.

In contrast to 4,7-dimethylindene, 3-phenyl-4,6-dimethylindene also reacted with acetone in KOH and DME to afford 2,2-bis(1-phenyl-5,7-dimethyl-3-indenyl)propane in 63% yield (Table 2).

Reaction Mechanism. We rationalize the failure of 4,7-methylindene to undergo coupling with acetone as follows. The reaction of indenyl anion (**8**, R = H) and acetone yields a fulvene intermediate (**10**, R = H). The intermediate has been isolated in many cases (see below) and subjected to the same reaction conditions to yield the coupling product. We also discovered that the failure of 4,7-dimethylindene to produce 2,2-bis(4,7-dimethyl-3-indenyl)propane (**11**, R = CH_3) results from the inability to produce intermediates **9** (R = CH_3) and **10** (R = CH_3) because of the equilibrium between **8** (R = CH_3) and **9** (R = CH_3).

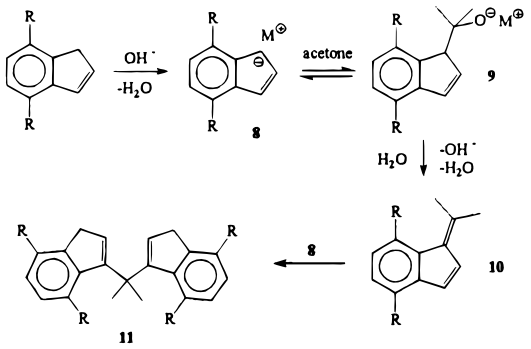

(3)

Employing a strong oxygen-affinitive magnesium as a countercation of **9** shifts the equilibrium of indenyl anion **8** (R = CH_3) and alkoxy anion **9** (R = CH_3) toward the latter (eq 4). The trap of alkoxyanion **9** (R = CH_3) leads to the isolation of the fulvene **10** (eq 5), which was converted to **11,** albeit in low yield.

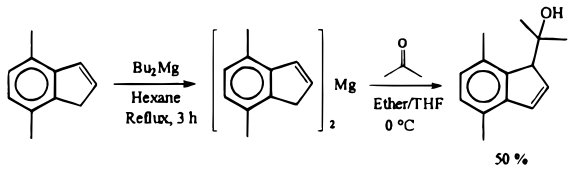

(4)

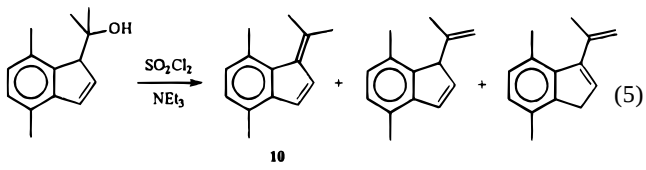

(5)

Since a primary alkoxy anion is less basic and more stable than a tertiary alkoxy anion, substituting formaldehyde for acetone (in eq 3) makes conversion of 4,7-dimethylindene into bis(4,7-dimethyl-3-indenyl)methane possible even under milder reaction conditions.

In an effort to prove the mechanism of the reaction, we successfully isolated the intermediate, 4,7-dimethyl-1-(phenylmethylidine)indene, in 86% yield in the reaction of 4,7-dimethylindene with benzaldehyde. This fulvene intermediate was further treated with indenyl anion to yield (indenyl)(phenyl)(4,7-dimethyl-1-indenyl)-methane **12** in 63% yield together with a small amount of 1-(phenylmethylidine)indene as a result of equilibrium, as shown in eq 6.

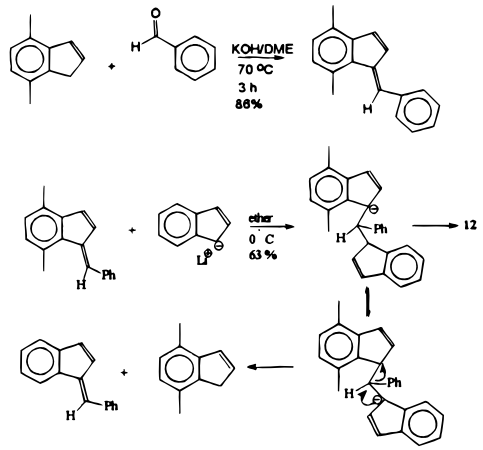

(6)

Synthesis of the Zirconocenes. The synthesis of the zirconocenes is straightforward. Both the dipotassium ligand salt in THF[8] and the dilithium ligand salt in Et_2O/pentane[9] can be conveniently used. The synthesis of two representative zirconocenes, that is, *rac*-$CH_2(Ind)_2ZrCl_2$ (**1**) and *rac*-$CH_2(4,7\text{-}Me_2\text{-}Ind)_2ZrCl_2$ (**2**), are reported in the Experimental Section. Although yields were somewhat low (for example, **1** and **2** were obtained in 9% and 23.2% yield, respectively, after crystallization), all metallocenes were obtained in high chemical and diastereomeric purity: only the racemic isomers were isolated (Chart 1).

Crystal and Molecular Structures of *rac*-Dichloro[methylenebis(η^5-1-indenyl)]zirconium (1), *rac*-Dichloro[methylenebis(4,7-dimethyl-η^5-1-indenyl)]-zirconium (2), and *rac*-Dichloro[isopropylidenebis-(η^5-1-indenyl)]zirconium (3). The racemic nature of compounds **1**, **2**, and **3** has been confirmed by X-ray analysis. Figures 1, 2, and 3 show (each) two different ORTEP views of **1**, **2**, and **3**, respectively. Tables 3 (lengths) and 4 (angles) contain the most relevant bonding parameters for the three compounds. Table 5 collects the angles between some relevant least-squares planes, a few slip-fold indicators, and the geometrical parameters described in Figure 4, for compounds **1**−**6**.

Compounds **1**−**3** are isomorphous and crystallize in the monoclinic space group *I*2/*c* (Table 6) with a crystallographically imposed 2-fold symmetry (the molecules lying about the Wycoff position 4*e*). Differences in cell parameters and volume can be easily explained considering the additional steric demand of the methyl substituents in **2** and **3**, with respect to **1**.

The zirconium atoms are pseudo-tetrahedrally coordinated by the two cyclopentadienyl groups of the bisindenyl moiety and by two chloro ligands. As usual for bent metallocenes, the overall coordination environment is best described by the set of parameters reported in Figure 4, which can be related to zirconium accessibility. In particular, the smaller the "bite angle" θ and the bigger the cp−Zr−cp′ φ one, the more the metal is tucked in the metal envelope.

(7) Luttikhedde, H. J. G.; Leino, R.; Wilén, C.-E.; Laine, E.; Sillanpää, R.; Näsman, J. H. *J. Organomet. Chem.* **1997**, *547*, 129.

(8) Grossman, R.; Doyle, R. A.; Buchwald, S. *Organometallics* **1991**, *10*, 1501.

Chart 1.[a]

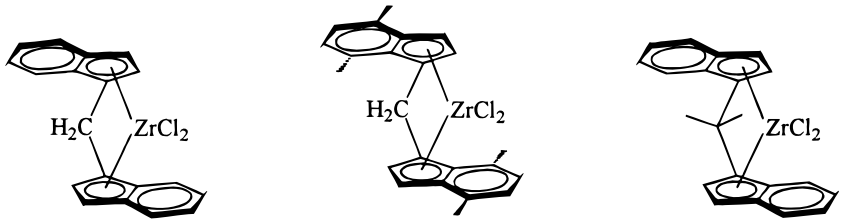

1 *rac*-$CH_2(Ind)_2ZrCl_2$ **2** *rac*-$CH_2(4,7\text{-}Me_2\text{-}Ind)_2ZrCl_2$ **3** *rac*-$Me_2C(Ind)_2ZrCl_2$

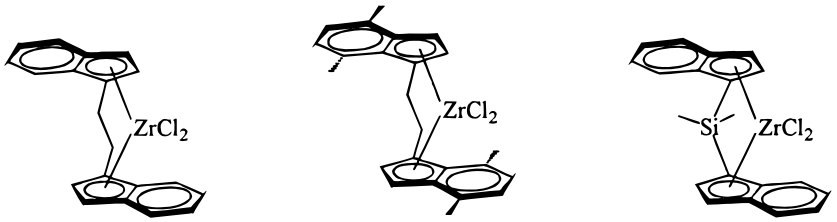

4 *rac*-$C_2H_4(Ind)_2ZrCl_2$ **5** *rac*-$C_2H_4(4,7\text{-}Me_2\text{-}Ind)_2ZrCl_2$ **6** *rac*-$Me_2Si(Ind)_2ZrCl_2$

[a] Only the *R*,*R* enantiomer is shown for each racemic mixture.

Table 3. Bond Lengths (Å)[a]

	1	2	3
Zr(1)−cp(1)	2.2123(18)	2.216(2)	2.2069(17)
Zr(1)−Cl(1)	2.4215(6)	2.4184(7)	2.4241(5)
Zr(1)−C(1)	2.4357(18)	2.447(2)	2.4347(17)
Zr(1)−C(2)	2.4618(18)	2.434(2)	2.4508(18)
Zr(1)−C(3)	2.5624(19)	2.538(2)	2.5483(18)
Zr(1)−C(3a)	2.6259(18)	2.631(2)	2.6142(17)
Zr(1)−C(7a)	2.5186(17)	2.562(2)	2.5332(17)
C(1)−C(2)	1.418(3)	1.415(3)	1.422(3)
C(1)−C(7a)	1.435(3)	1.430(4)	1.443(2)
C(1)−C(8)	1.509(3)	1.516(3)	1.533(2)
C(2)−C(3)	1.400(3)	1.397(3)	1.397(3)
C(3)−C(3a)	1.415(3)	1.411(3)	1.407(3)
C(3a)−C(4)	1.416(3)	1.427(4)	1.424(3)
C(3a)−C(7a)	1.447(3)	1.442(4)	1.446(2)
C(4)−C(5)	1.359(3)	1.351(5)	1.345(3)
C(4)−C(9)		1.494(5)	
C(5)−C(6)	1.412(3)	1.409(6)	1.421(3)
C(6)−C(7)	1.355(3)	1.367(5)	1.352(3)
C(7)−C(7a)	1.425(3)	1.447(4)	1.428(2)
C(7)−C(10)		1.501(5)	
C(8)−C(9)			1.531(3)

[a] cp refers to the centroid of the five-member ring of the organic ligand.

Table 4. Selected Bond Angles (deg)[a]

	1	2	3
cp(1)−Zr(1)−Cl(1)	109.23(2)	108.69(2)	108.72(2)
cp(1)−Zr(1)−cp(1′)	117.38(3)	117.07(3)	118.06(3)
cp(1)−Zr(1)−Cl(1′)	110.15(2)	111.05(2)	109.98(2)
Cl(1)−Zr(1)−Cl(1′)	99.18(3)	98.77(4)	99.85(3)
C(2)−C(1)−C(7a)	106.67(18)	106.6(2)	105.87(16)
C(2)−C(1)−C(8)	124.74(18)	121.9(2)	123.43(15)
C(7a)−C(1)−C(8)	125.87(16)	128.8(2)	128.34(14)
C(1)−C(2)−C(3)	109.79(19)	110.3(2)	110.46(17)
C(2)−C(3)−C(3a)	108.48(19)	107.6(2)	108.09(16)
C(3)−C(3a)−C(4)	133.20(19)	129.5(3)	131.78(18)
C(3)−C(3a)−C(7a)	107.19(18)	108.0(2)	107.91(16)
C(4)−C(3a)−C(7a)	119.61(18)	122.5(2)	120.31(18)
C(3a)−C(4)−C(5)	119.1(2)	115.9(3)	119.05(19)
C(3a)−C(4)−C(9)		119.8(3)	
C(5)−C(4)−C(9)		124.2(3)	
C(4)−C(5)−C(6)	121.7(2)	122.8(3)	121.25(19)
C(5)−C(6)−C(7)	121.4(2)	124.1(3)	121.90(19)
C(6)−C(7)−C(7a)	119.45(19)	115.9(3)	119.57(18)
C(6)−C(7)−C(10)		121.6(3)	
C(7a)−C(7)−C(10)		122.4(4)	
C(1)−C(7a)−C(3a)	107.82(17)	107.5(2)	107.63(16)
C(1)−C(7a)−C(7)	133.45(19)	133.7(3)	134.46(17)
C(3a)−C(7a)−C(7)	118.73(19)	118.8(3)	117.91(16)
C(1)−C(8)−C(9)			113.59(11)
C(1)−C(8)−C(1′)	101.4(2)	101.8(3)	99.73(19)
C(1)−C(8)−C(9′)			111.41(12)
C(9)−C(8)−C(9′)			107.2(3)

[a] Primes address symmetry-equivalent atoms ($-x$, y, $1/2 - z$).

As can be seen from the values reported in Table 5, these parameters are very sensitive to differences in the number and type of the *ansa* atoms, while the presence of substituents on the ligand moiety leads to minor changes in the *local* stereochemistry of the metal atom. As a consequence, the only noticeable difference between parameters for compounds **1**−**3** consists of a slightly more open angle α (hence a more open θ one) for methylene-bridged molecules (**1** and **2**) with respect to the isopropylidene-bridged one (**3**).

On comparing the present *ansa*-1C molecules to the related *ansa*-2C one, we notice that the presence of a shorter bridge affects the spread of the Zr−C interactions (which display a 1 > 2 > 2 pattern instead of a 2 > 2 > 1 one) since one of the two bridgehead atoms, namely C(7a), which normally suffers from the indenyl ring slippage, is bound to be closer to the zirconium atom.

The presence of methyl substituents at the benzene rings or at the *ansa* atom in **2** and **3** gives rise to some additional molecular strain, and to relieve unfavorable steric interactions, the indenyl ligands bend away from the bridging moiety by means of a lengthening of the Zr−C(3a) and Zr−C(7a) bonds (and a parallel shortening of the Zr−C(2) and Zr−C(3) ones), together with an increased deviation from planarity (see the *al*−*bz* and Ω values in Table 5).

Table 5. Relevant Geometrical Parameters[a]

	1	2	3	4	5	6
α	101.4	101.8	99.7			94.6
β	84.8	84.5	85.0	84.6	85.8	84.8
γ	14.5	14.9	14.4			16.3
θ	72.4	71.5	70.9	62.1	59.9	61.8
φ	117.4	117.1	118.1	126.9	125.3	127.8
al−*bz*	2.2	5.1	2.4	5.4	5.7	3.4
$ZrCl_2$−*cp*	36.2	35.8	35.5	31.1	30.1	31.0
bh−*cp*−*cp*′−*bh*′	150.8	150.6	149.2	138.1	143.7	147.7
Ω	1.3	1.6	1.9	2.3	1.5	1.7
Δ	0.20	0.21	0.19	0.21	0.16	0.20

[a] All quantities in degrees, apart from Δ (Å). The angles α, *β*, *γ*, *θ*, and *φ* are defined in Figure 4. *al*, *bz*, *cp*, and $ZrCl_2$ refer to the least-squares planes defined by the allylic moiety [C(1), C(2), C(3)], the aromatic six-member ring, the five-member ring, and the $ZrCl_2$ atoms, respectively. *bh* refers to the centroid of the bridgehead atoms [C(3a) and C(7a)]. Ω is the angle between the plane defined by the allylic moiety and the least-squares plane defined by the atoms C(1), C(7a), C(3a), and C(3); Δ is the distance between the perpendicular projection of the heavy atom on the ring least-squares plane and the ring centroid.

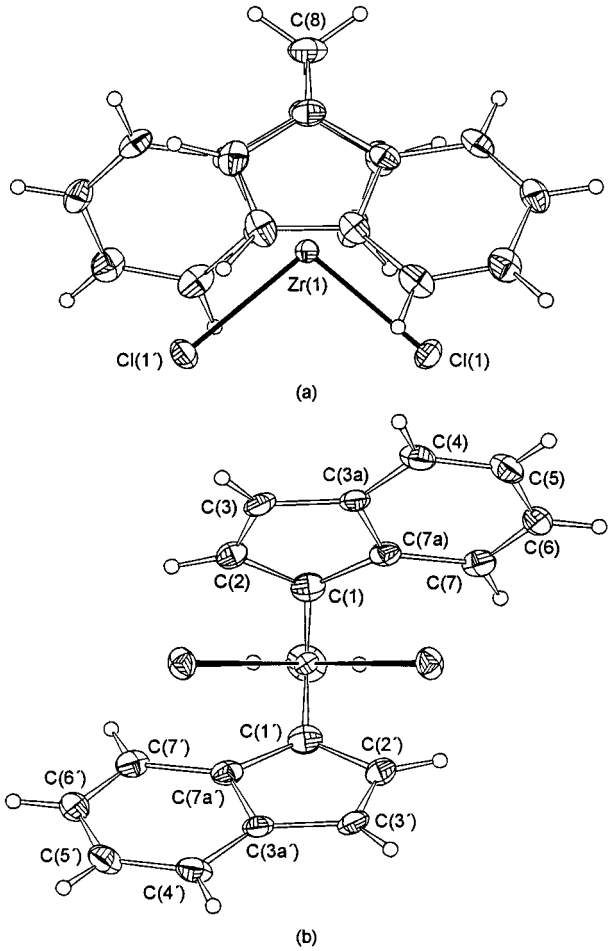

Figure 1. Top (a) and front (b) ORTEP views of **1**. Displacement ellipsoids are drawn at the 30% probability level. Hydrogen atoms are given arbitrary radii.

Moreover, in **2** and **3** the steric demand of the methyl substituents determines a marked distortion of the indenyl moiety *within* its average plane, recognizable by comparing "equivalent" bond angles at the bridgehead carbon atoms: C(3)−C(3a)−C(4) vs C(1)−C(7a)−C(7) and C(4)−C(3a)−C(7a) vs C(3a)−C(7a)−C(7) (129.5° vs 133.7° and 122.5° vs 118.8° in **2**; 131.8° vs 134.5° and 120.3° vs 117.9° in **3**). At variance, in **1** these angles (133.4° vs 133.2° and 119.6° vs 118.7°) are more similar.

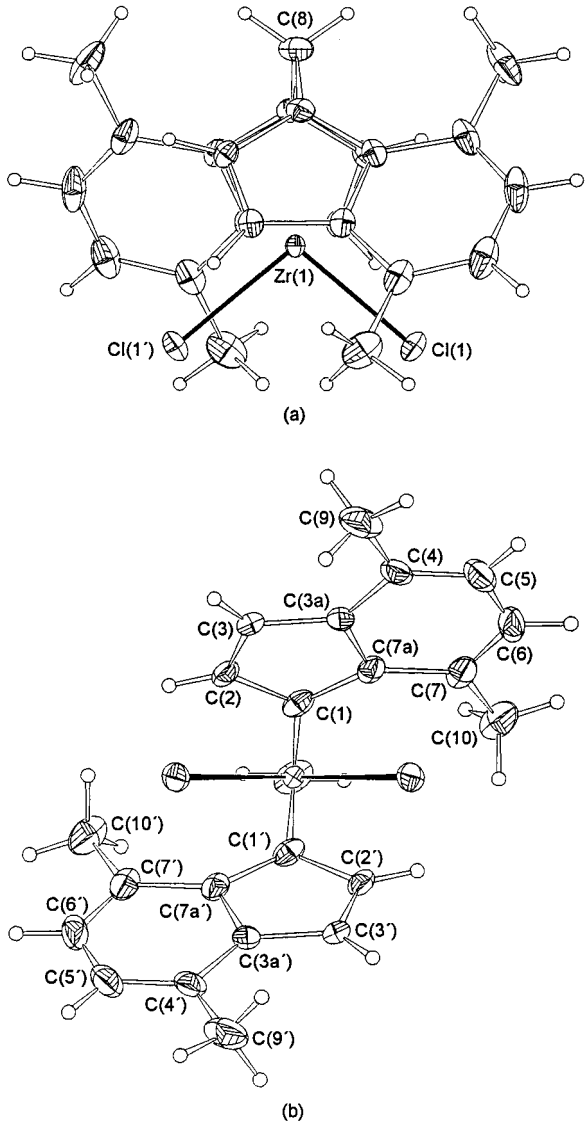

Figure 2. Top (a) and front (b) ORTEP views of **2**. Displacement ellipsoids are drawn at the 30% probability level. Hydrogen atoms are given arbitrary radii.

According to an adaptation by Schlogl of the Cahn−Ingold−Prelog rules, the stereoisomers represented in Figures 1, 2, and 3 have an *S*,*S* configuration at C(1) and C(1′), respectively. However, both in solution and in the solid state, as they crystallize in a centrosymmetric space group, their *R*,*R* enantiomers are also present.

Polymerizations

As representative examples of methylene-bridged zirconocenes, we tested *rac*-$CH_2(Ind)_2ZrCl_2$ (**1**) and *rac*-$CH_2(4,7\text{-}Me_2\text{−}Ind)_2ZrCl_2$ (**2**), in both ethylene and propylene polymerization, and compared them to the available isopropylidene-, ethylene-, and dimethylsilylene-bridged analogues.

Ethylene Polymerization

The results are reported in Table 7. Both polymerization activities and PE molecular weights depend on

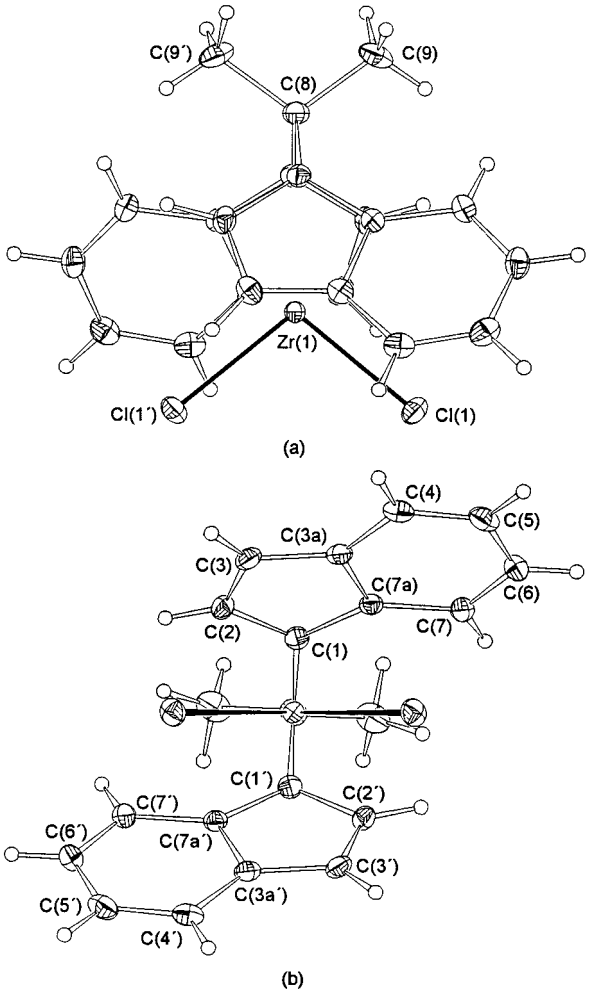

Figure 3. Top (a) and front (b) ORTEP views of **3**. Displacement ellipsoids are drawn at the 30% probability level. Hydrogen atoms are given arbitrary radii.

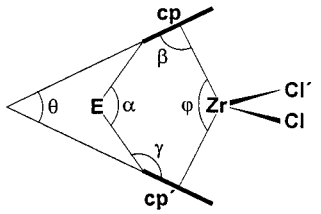

Figure 4. Schematic representation of an *ansa*-zirconocene molecule detailing the angles listed in Table 5. α is the angle C(1)−E−C(1′); β is the angle between the Zr−*cp* vector and the *cp* least-squares plane; γ is the angle between the C(1)−E vector and the *cp* least-squares plane; θ is the angle between the least-squares planes of the two cyclopentadienyl ligands; and φ is the angle *cp*−Zr−*cp′*.

both the type of bridge and the substitution on the indenyl groups. We first analyze the series of the four unsubstituted bisindenyl complexes with CH_2 (**1**), Me_2C (**3**), C_2H_4 (**4**), and Me_2Si (**6**) bridges, for which we can compare the structural parameters (see Table 5). Activities increase, within an order of magnitude, in the order **1** < **3** < **4** < **6**, following the decrease in the value of the "bite angle", θ. We can rationalize this effect by assuming that a smaller bite angle reduces the formation of deactivated bimetallic species.[11] For the same series, the average viscosity molecular weight increases 5-fold on going from **1** to **6**, following the same order of decreasing θ. End-group analysis by ^{1}H NMR of PE from **1**−**3** shows the presence of vinyl end groups, indicating β-H transfer, likely to the monomer, and a minor amount of vinylidene in the case of **1** and **2**, very likely arising from reinsertion of an ethylene macromer into a growing polyethylene chain (Scheme 1). The proton spectrum of the olefin region of the PE sample from *rac*-CH_2(4,7-Me_2−Ind_2ZrCl_2 is shown in Figure 5, and the relative composition of end groups in Table 8.

This mechanism has been invoked to explain long-chain-branching formation in PE from both the Ti-"constrained geometry" catalyst and metallocene catalysts and observed with a mixed catalyst system.[12]

Traces of vinylenes are also present. These are assigned to an internal vinylene structure, possibly arising from β-H transfer after a secondary insertion of the vinyl-terminated ethylene macromer.[13] Assuming that β-H transfer is the main chain transfer reaction for all zirconocene catalysts investigated here, the decrease of molecular weight for larger values of θ can be rationalized in terms of a decrease in nonbonded interactions in the conformation of the growing chain leading to β-H transfer.

The same trend observed for **4** and **1** can be seen by comparing **5** and **2**: on going from the ethylene to the methylene bridge, we obtain lower molecular weight and lower catalyst activity. The second factor that affects catalyst activity and PE molecular weight is indenyl substitution. By increasing the number of substituents, catalyst activity increases in the order **1** < **2** (the same happens in the case of **4** vs **5**), while molecular weight is only marginally influenced. This important aspect will be further investigated on a larger set of catalysts and reaction conditions. The results of thermal analysis are consistent with the molecular weight data: in particular, increasing molecular weights causes a slight increase in the melting temperature and a decrease in the heat of fusion (crystallinity).[14]

Propylene Polymerization

Selected results of propylene polymerization with **1** and **2**, in comparison to zirconocenes with different bridges, are shown in Table 9. These methylene-bridged C_2-symmetric, isospecific zirconocenes show a significant variation in propylene polymerization performance with

(9) Resconi, L.; Jones, R. L.; Rheingold, A. L.; Yap, G. P. A. *Organometallics* **1996**, *15*, 998.

(10) Flory, P. J. *Principles of Polymer Chemistry*; Cornell University Press: Ithaca, NY, 1953.

(11) Bochmann, M.; Lancaster, S. J. *J. Organomet. Chem.* **1995**, *497*, 55. Haselwander, T.; Beck, S.; Brintzinger, H.-H. In *Ziegler Catalysts*; Fink, G., Mülhaupt, R., Brintzinger, H.-H., Eds.; Springer-Verlag: Berlin, 1995; p 181. Yang, X.; Stern, C. L.; Marks, T. J. *J. Am. Chem. Soc.* **1994**, *116*, 10015.

(12) Swogger, K. W. In *Catalyst Design for Taylor-Made Polyolefins, Studies in Surface Science Catalysis;* Soga, K., Terano, M., Eds.; Kodansha-Elsevier: Tokyo, 1994; Vol. 89, p 285. Soga, K.; Uozumi, T.; Nakamura, S.; Toneri, T.; Teranishi, T.; Sano, T.; Arai, T. *Macromol. Chem. Phys.* **1996**, *197*, 4237. Malmberg, A.; Kokko, E.; Lehmus, P. Löfgren, B.; Seppälä, J. V. *Macromolecules* **1998**, *31*, 8448. Barnhart, R. W.; Bazan, G. C.; Mourey, T. *J. Am. Chem. Soc.* **1998**, *120*, 1082.

(13) Karol, F. J.; Kao, S.; Wasserman, E. P.; Brady, R. C. *New J. Chem.* **1997**, *21*, 797. Wasserman, E.; Hsi, E.; Young, W.-T. *Polym. Prepr. Am. Chem. Soc., Div. Polym. Chem.* **1998**, *39* (2), 425.

(14) (a) van der Ven, S. In *Study in Polymer Science 7, Polypropylene and other Polyolefins, Polymerization and Characterization*; Elsevier: Amsterdam, 1990; p 470. (b) Mandelkern, L. *Acc. Chem. Res.* **1990**, *23*, 380.

Table 6. Summary of Crystal Data, Data Collection, and Structure Refinement Parameters

	1	2	3
Crystal Data			
formula	$C_{19}H_{14}Cl_2Zr$	$C_{23}H_{22}Cl_2Zr$	$C_{21}H_{18}Cl_2Zr$
fw	404.42	460.53	432.47
crystal system	monoclinic	monoclinic	monoclinic
space group	*I*2/*c* (No. 15)	*I*2/*c* (No. 15)	*I*2/*c* (No. 15)
a (Å)	11.632(3)	11.913(3)	11.506(1)
b (Å)	9.988(1)	11.984(2)	11.128(1)
c (Å)	14.162(3)	13.919(2)	13.969(1)
β (deg)	103.00(1)	99.57(2)	103.31(1)
V (Å^3)	1603.2(5)	1959.5(7)	1740.5(3)
Z	4	4	4
F(000)	808	936	872
density (g cm^{-3})	1.676	1.561	1.650
absorption coeff (mm^{-1})	1.011	0.838	0.937
crystal description	red prism	orange block	orange block
crystal size (mm)	0.26 × 0.14 × 0.12	0.20 × 0.16 × 0.16	0.20 × 0.18 × 0.16
Data Collection			
diffractometer	Siemens SMART	Enraf-Nonius CAD-4	Enraf-Nonius CAD-4
scan mode	ω	ω	ω
θ range (deg)	$2.5 \le \theta \le 26.8$	$3.4 \le \theta \le 25.0$	$3.6 \le \theta \le 27.0$
index ranges	$-13 \le h \le 14$ $-7 \le k \le 12$ $-17 \le l \le 15$	$-14 \le h \le 13$ $0 \le k \le 14$ $0 \le l \le 16$	$-14 \le h \le 14$ $0 \le k \le 14$ $0 \le l \le 17$
intensity decay (%)	none	none	none
absorption correction	SADABS	ψ scan	ψ scan
transmission factors (min, max)	0.672, 0.886	0.833, 0.874	0.832, 0.861
no. of measured reflns	4068	1716	1982
no. of ind reflns	1545	1716	1902
R_{int}, R_σ[α]	0.0156, 0.0246	−, 0.0239	0.0104, 0.0167
no. of reflns with $I > 2\sigma(I)$	1373	1445	1666
Refinement			
no. of data/restraints/params	1545/0/101	1445/0/121	1666/0/111
weights (*a*, *b*)[b]	0.026, 0	0.027, 1.26	0.034, 0.56
goodness-of-fit $S(F^2)$[c]	0.910	1.082	1.134
$R(F)$, $I > 2\sigma(I)$[d]	0.0185	0.0213	0.0199
$wR(F^2)$, all data[e]	0.0432	0.0509	0.0538
largest diff peak, hole (e Å^{-3})	0.251, −0.317	0.196, −0.175	0.236, −0.381

[a] $R_{int} = \sum|F_o^2 - F_{mean}^2|/\sum|F_o^2|$; $R_\sigma = \sum|\sigma(F_o^2)|/\sum|F_o^2|$. [b] $w = 1/[\sigma^2(F_o^2) + (aP)^2 + bP]$, where $P = (F_o^2 + 2F_c^2)/3$. [c] $S = [\sum w(F_o^2 - F_c^2)^2/(n - p)]^{1/2}$, where *n* is the number of reflections and *p* is the number of refined parameters. [d] $R(F) = \sum||F_o| - |F_c||/\sum|F_o|$. [e] $wR(F^2) = [\sum w(F_o^2 - F_c^2)^2/\sum wF_o^4]^{1/2}$.

Table 7. Polymerization of Ethylene[a]

zirconocene (racemic)	Zr (μmol)	activity (kg_{PE}/($mmol_{Zr}$ h))	$[\eta]$[b] (dL/g)	$\bar{M}_v$[c] × 10^{-4}	T_m[d] (°C)	ΔH (J/g)
1 $CH_2(Ind)_2ZrCl_2$	0.25	6.9	0.9	4.5	130	206
2 $CH_2(4,7\text{-}Me_2\text{-}Ind)_2ZrCl_2$	0.43	22.8	1.1	5.9	131	191
3 $Me_2C(Ind)_2ZrCl_2$	0.34	10.0	1.36	8.0	131	190
4 $C_2H_4(Ind)_2ZrCl_2$	0.24	53.8	2.0	13.6	137	152
5 $C_2H_4(4,7\text{-}Me_2\text{-}Ind)_2ZrCl_2$	0.21	67.5	2.6	19.5	138	178
6 $Me_2Si(Ind)_2ZrCl_2$[e]	0.22	62.0	3.0	23.7	138	175

[a] Hexane, T_p = 80 °C, 4.2 bar ethylene, 10 min; MAO cocatalyst, Al/Zr = 1000 mol/mol. MAO was dried in vacuo to a free-flowing powder. [b] Measured in THN at 135 °C. [c] Obtained from $[\eta] = K(M_v)^\alpha$ with $K = 3.8 \times 10^{-4}$ and $\alpha = 0.725$.[9] [d] Peak melting temperature of the second melting (heating rate 10 °C/min). [e] 5 min, T_p = 75 °C.

Scheme 1. Formation of Vinylidenes in Polyethylene

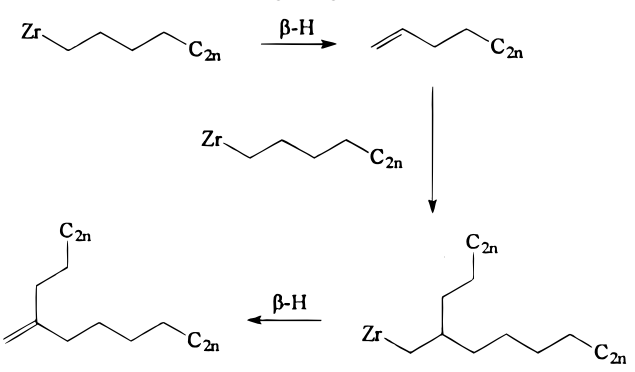

respect to their ethylene- (**4**, **5**), isopropylidene- (**3**), or dimethylsilylene-bridged (**6**) congeners. In fact, both **1**/MAO and **2**/MAO produce isotactic polypropylenes, which have both lower molecular weight and lower isotacticity than those obtained from **3**−**6**/MAO. **1**/MAO and **2**/MAO, for example, produce waxy materials with degree of oligomerization ∼70 and T_m ∼110−120 °C. The X-ray analysis of **1** and **2** has shown that their molecular structures are more open (larger θ, smaller φ angles) than their analogues with other bridges. This structural feature results in a lower isotacticity of *i*-PP (Table 9). Regioselectivity does not seem to be influenced in the series of complexes with unsubstituted indenes, while **2** is more regiospecific than **5**, reflecting a minor nonbonded interaction between the incoming propylene molecule and the 4-methyl group. At the same time, as in the case of ethylene polymerization, **1** and **2** produce polypropylenes with lower molecular weights than **3**−**6**. The end-group analysis of *i*-PP samples from **1**−**6** is

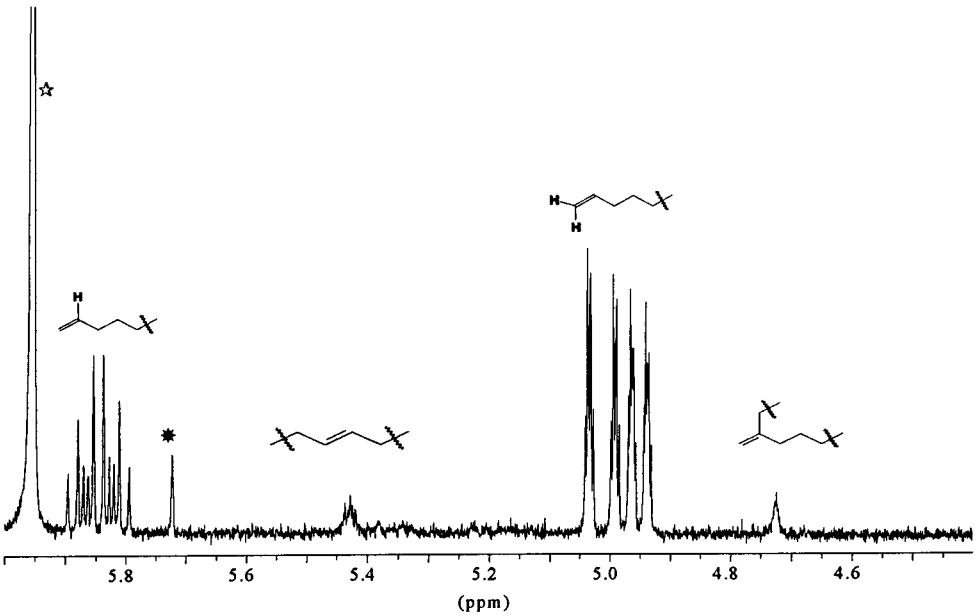

Figure 5. ^{1}H NMR spectra of the olefin region of HDPE from **2**/MAO. ☆ peak due to residual C_2HDCl_4 (reference at 5.95 ppm) and ★ solvent impurity.

Table 8. Molecular Weight Data and Unsaturated End Group Composition of Polyethylenes from Racemic Zirconocene/MAO Catalysts: Dependence on Structural Parameters

rac-Zirconocene	θ (°)	φ (°)	$\bar{P}_n$ [a]	$\bar{P}_n$ [b]	vinyl	intern. vinylene	vinylidene
1	72.4	117.4	800	633	91.9	traces	8.1
2	71.5	117.1	1050	784	89.4	6.6	4.0
3	70.9	118.1	1430	1510	100	traces	-
4	62.1	126.9	2430	3050	100	traces	-
5	59.9	125.3	3480	n.d	n.d	n.d	n.d.
6	61.8	127.8	4230	n.d.	n.d.	n.d.	n.d.

[a] From intrinsic viscosity, assuming $\bar{M}_v = \bar{M}_w = 2\bar{M}_n$. [b] From ^{1}H NMR, assuming one double bond per chain and no transfer to Al.

Table 9. Polymerization of Propylene[a]

zirconocene (racemic)	μmol	Al/Zr (M)	activity (kg_{PP}/($mmol_{Zr}$ h))	*mmmm* (%)	2,1 (%)	$[\eta]^b$ (dL/g)	T_m (°C)	ΔH (J/g)
1	1.2	4000	62.0	71.4	0.5	~0.1	110	68
2	2.5	2000	23.5	85.8	0.8	<0.1	122	81
3	2.3	3000	65.8	80.7	0.4	~0.2	127	77
4	0.5	8000	152.0	87.3	0.6	0.44	134	80
5	2.1	2000	71.8	92.3	1.9	~0.1	131	88
6	0.2	38000	198.0	90.3	0.5	0.63	144	84

[a] Liquid propylene, T_p = 50 °C, 1 h, MAO cocatalyst. 2,1 is the total secondary insertions in the chain (end groups not included). [b] Measured in THN at 135 °C.

reported in Table 10, together with the average degree of polymerization, $\bar{P}_n$, estimated from the unsaturated end groups, in the hypothesis of one double bond per chain and no chain transfer to Al. Since the most important unsaturated end groups are 2-butenyl and vinylidene, the two relevant chain-transfer reactions are primary and secondary β-hydride transfers.[15] The proton spectra of the olefin region of the *i*-PP samples from **1**−**5** are compared in Figure 6. In Table 10 we report also the relative frequency of the 2-butenyl and vinylidene end groups (end group per inserted propylene unit).

We observe a correlation between $\bar{P}_n$ and both θ and φ, showing the direct influence of the bite angle on the facility of β-H transfer reactions: the four members in the series of the simple bisindenyl complexes **1**, **3**, **4,** and **6** show a decrease of both the relative rate of secondary and primary β-H transfer reactions, with decreasing values of θ.

Conclusions

We have described an inexpensive and atom-efficient protocol for the synthesis of bis(indenyl)methanes, via the base-catalyzed condensation between formaldehyde and (substituted) indenes in polar solvents such as DMF or DMSO. This method can be applied to alkylated indenes, and even to fluorene, providing a facile entry

(15) Resconi, L.; Camurati, I.; Sudmeijer, O. *Top. Catal.* **1999**, *7* (1−4), 145.

Table 10. Unsaturated End Group Composition and Frequency of Chain-Transfer Reactions in Polypropylenes from Racemic Zirconocene/MAO Catalysts: Dependence on Structural Parameters

Zirconocene	θ (°)	φ (°)	$\bar{P}_n$ [a]	vinylidene %	vinylidene f(×10³)	intern. vinylid.	2-butenyl %	2-butenyl f(×10³)	2-butenyl isomer
1	72.4	117.4	74	82.1	11	0	17.9	2.4	cis/trans
2	71.5	117.1	73	49.9	6.8	0	50.1	6.8	cis
3	70.9	118.1	170	75.9	4.4	6.0	18.1	1.1	cis/trans
4	62.1	126.9	546 [b]	29.5 [c]	0.5	12.8 [c]	48.0 [c]	0.9	cis
5	59.9	125.3	108 [b]	1.2 [d]	0.09	0.4 [d]	90.9 [d]	8.1	cis
6	61.8	127.8	891	32.9	0.5	20.9	46.2	0.6	cis

[a] From ^{1}H NMR, assuming one double bond per chain and no transfer to Al, and not considering the internal vinylidene. Frequencies are defined as end groups per monomer unit. [b] Average values. [c] 9.7% triplet at 5.2 ppm. [d] 5.5% triplet at 5.2 ppm, ca. 2% peaks at 4.9−5.1 ppm.

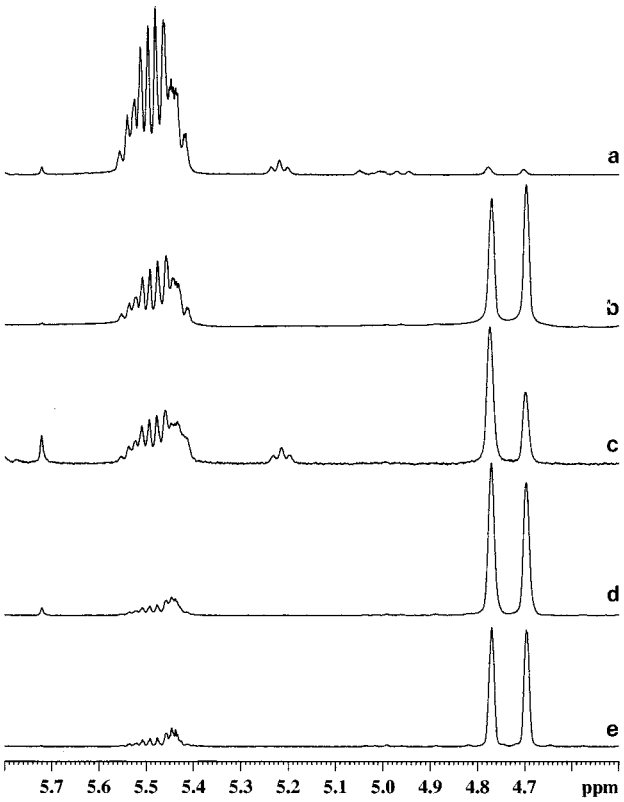

Figure 6. ^{1}H NMR spectra of the olefin region of *i*-PP samples from (a) **5**/MAO, (b) **2**/MAO, (c) **4**/MAO, (d) **3**/MAO, and (e) **1**/MAO.

into methylene-bridged *ansa*-zirconocenes. The methylene-bridged chiral zirconocenes, investigated in this work, produce vinyl-terminated low molecular weight polyethylenes, and polypropylene waxes with lower molecular weights and lower isotacticities than their closer analogues. In fact, both **1**/MAO and **2**/MAO produce isotactic oligopropylenes, which have both lower molecular weight and lower isotacticity than those obtained from *rac*-$C_2H_4(Ind)_2ZrCl_2$/MAO and *rac*-C_2H_4-$(4,7\text{-}Me_2Ind)_2ZrCl_2$/MAO. **2**/MAO, for example, produces *i*-PP with degree of oligomerization ~70. The products are waxy materials with $T_m \approx 110-120$ °C.

Experimental Section

General Procedures. All reactions were performed under nitrogen. Anhydrous solvents (Aldrich) were used without further purification. ^{1}H NMR spectra were recorded on a Varian Unity 300 instrument. Chemical shifts (δ) are in ppm downfield from tetramethylsilane as internal standard. Mass spectra were recorded at 70 eV on a Hewlett-Packard 5890 GC/MSD instrument. Preparations of the zirconocenes were performed under nitrogen by using conventional Schlenk-line techniques. Solvents were distilled from blue Na−benzophenone ketyl (THF, Et_2O), CaH_2 (CH_2Cl_2), or Al(*i*-Bu)$_3$ (hydrocarbons) and stored under nitrogen. KH, MeLi, and BuLi (Aldrich) were used as received. All NMR solvents were dried over $LiAlH_4$ or CaH_2 and distilled before use. Polymerization grade ethylene and propylene were received directly from the Montell Ferrara plant. MAO (Witco, 10% w/w in toluene) was used as received. The zirconocenes *rac*-$Me_2C(Ind)_2ZrCl_2$,[16] *rac*-$C_2H_4(Ind)_2ZrCl_2$,[17] *rac*-$C_2H_4(4,7\text{-}Me_2\text{-}Ind)_2ZrCl_2$,[18] and *rac*-$Me_2Si(Ind)_2ZrCl_2$[19] were prepared according to literature procedures. All were characterized as reported in the literature and gave satisfactorily elemental analyses.

Bis(4,7-dimethyl-3-indenyl)methane. Formalin (37% solution, 0.28 g, 3.47 mmol) was added to a mixture of 4,7-dimethylindene (1.0 g, 6.94 mmol) and sodium ethoxide (0.15 g, 2.20 mmol) in dimethyl sulfoxide (10 mL). The reaction mixture was stirred at room temperature for 12 h and then at 80 °C for another 4 h and cooled to room temperature; then HCl (1 M, 10 mL) was added. The mixture was extracted with CH_2Cl_2 (2 × 50 mL). The organic phases were combined, washed with brine and then with water, dried ($MgSO_4$), and concentrated to yield a brown solid. A yellow solid was obtained after washing with MeOH (0.52 g, 50%). The yield of a similar reaction in DMF was 48%.

Analogously, paraformaldehyde (2.08 g, 69.4 mmol) was added to a mixture of 4,7-dimethylindene (25.0 g, 174 mmol) and sodium ethoxide (5.9 g, 87 mmol) in dimethyl sulfoxide (200 mL). After stirring at room temperature for 12 h, the reaction mixture was heated at 65 °C for another 8 h. It was then cooled to room temperature. Hydrochloric acid (1 M, 400 mL) was added. The mixture was extracted with CH_2Cl_2 (400

(16) Spaleck, W.; Antberg, M.; Dolle, V.; Klein, R.; Rohrmann, J.; Winter, A. *New J. Chem.* **1990**, *14*, 499.
(17) Wild, F.; Wasiucionek, M.; Huttner, G.; Brintzinger, H. H. *J. Organomet. Chem.* **1985**, *288*, 63.
(18) Resconi, L.; Piemontesi, F.; Camurati, I.; Balboni, D.; Sironi, A.; Moret, M.; Rychlicki, H.; Zeigler, R. *Organometallics* **1996**, *15*, 5046.
(19) Spaleck, W.; Antberg, M.; Rohrmann, J.; Winter, A.; Bachmann, B.; Kiprof, P.; Behm, J.; Hermann, W. *Angew. Chem., Int. Ed. Engl.* **1992**, *31*, 1347.

mL). All organic layers were combined, washed with brine and then with water, dried ($MgSO_4$), and concentrated to yield a viscous brown liquid. GC analysis showed only product and starting material. No fulvene derivative was detected. Precipitation occurred when the brown liquid was added into pentane (100 mL). Bis(4,7-dimethyl-3-indenyl)methane (6.8 g, 33% yield) was obtained as a yellow solid after filtering and washing with pentane and EtOH successfully. ^{1}H NMR ($CDCl_3$): δ 6.85−7.05 (m, 4 H), 6.35 (s, 2 H), 4.20 (s, 2 H), 3.2 (s, 4 H), 2.55 (s, 6 H), 2.35 (s, 6 H).

Similar procedures were employed for the other compounds. The pure compounds were obtained by precipitation from methanol.

Bis(3-indenyl)methane. ^{1}H NMR ($CDCl_3$, δ, ppm): 7.10−7.60 (m, 8 H), 6.25 (s, 2 H), 3.85 (s, 2 H), 3.40 (s, 4 H).

Bis(1-tert-butyl-3-indenyl)methane. ^{1}H NMR ($CDCl_3$, δ, ppm): 7.7−7.1 (m, 8 H), 6.2 (s, 2 H), 3.8 (s, 2 H), 3.2 (s, 2 H), 1.0 (s, 18 H).

Bis(1-phenyl-5,7-dimethyl-3-indenyl)methane. ^{1}H NMR ($CDCl_3$, δ, ppm): 6.7−7.2 (m, 14 H), 6.25 (s, 2 H), 4.5 (s, 2 H), 3.8 (s, 2 H), 2.35 (s, 6 H), 2.0 (s, 6 H).

Bis(fluorenyl)methane. ^{1}H NMR ($CDCl_3$, δ, ppm) 7.2−7.8 (m, 16 H), 4.4 (t, 2 H, J = 7.6 Hz), 2.2 (t, 2 H, J = 7.6 Hz).

***rac*-CH_2(1-Ind)$_2ZrCl_2$ (1)**. A 2.135 g sample of bis(1-indenyl)methane (8.75 mmol) was dissolved in 30 mL of THF and slowly added to a stirred suspension of 0.8 g of KH (19.5 mmol) in 50 mL of THF in a 100 mL Schlenk tube. Evolution of H_2 ceases after 1 h 30 min, and the resulting brownish solution was separated from excess KH. This solution and a solution of $ZrCl_4(THF)_2$ (3.3 g, 8.75 mmol) in THF (80 mL) were both added dropwise via dropping funnels to a 250 mL flask containing rapidly stirring THF (20 mL) over 5.5 h. At the end of the addition the mixture was stirred overnight at room temperature. A yellow-orange solution and a precipitate formed. After concentrating the suspension under reduced pressure to about 10 mL, 10 mL of Et_2O were added, the suspension was filtered, and the residue was dried in vacuo and extracted with refluxing CH_2Cl_2 until the washing was colorless (2 h). The CH_2Cl_2 solution (part of the product precipitated during extraction) was concentrated to yield 2.135 g of red solid. This was washed with Et_2O (3 × 5 mL), 2 mL CH_2Cl_2, and again Et_2O, to give 1.06 g of the target compound with some organic impurities. Crystallization from toluene yielded 0.32 g (9.0%) of red-orange *rac*-CH_2(1-Ind)$_2ZrCl_2$ free of its meso isomer. ^{1}H NMR (CD_2Cl_2, δ, ppm): s, 4.87, 2 H, CH_2; d, 6.02−6.04, 2 H; d, 6.59−6.61, 2 H; three m, 7.1−7.7, 8H). Anal. Calcd for $C_{19}H_{14}Cl_2Zr$: C, 56.4; H, 3.5. Found: C, 56.9; H, 3.6.

***rac*-CH_2(4,7-Me_2-1-Ind)$_2ZrCl_2$ (2)**. A suspension of bis(4,7-dimethyl-indenyl)methane (2 g, 6.7 mmol) in THF (30 mL) was added via cannula to a stirred suspension of KH (0.6 g, 15 mmol) in THF (35 mL). After hydrogen evolution had ceased (2 h) the resulting brownish solution was separated from excess KH. This solution and a solution of $ZrCl_4(THF)_2$ (2.5 g, 6.7 mmol) in THF (65 mL) were both added dropwise via dropping funnels to a flask containing rapidly stirring THF (30 mL) over 4 h. At the end of the addition the mixture was stirred overnight. A brick-red solution and a precipitate formed. After concentrating in vacuo to about 4 mL, 10 mL of Et_2O was added, the suspension was filtered, and the residue was dried in vacuo (brown powder) and was extracted with refluxing CH_2Cl_2 until the washing was colorless. The CH_2Cl_2 solution was concentrated to 7 mL and cooled to −20 °C overnight. A red solid (0.715 g) was isolated by filtration. ^{1}H NMR showed the formation of the pure racemic isomer of methylenebis(4,7-dimethylindenyl)$ZrCl_2$. ^{1}H NMR ($CDCl_3$, δ, ppm): 6.99 (d, 2 H), 6. 76 (d, 2 H), 6.65 (d, 2 H), 5.88 (d, 2 H), 5.09 (s, 2 H), 2.76 (s, 6 H), 2.30 (s, 6 H). Anal. Calcd for $C_{23}H_{22}Cl_2Zr$: C, 60.0; H, 4.8. Found: C, 60.4; H, 4.9.

Polymerizations of Propylene. A 200 g sample of propylene was charged in a 1 L jacketed stainless steel autoclave, equipped with a magnetically driven stirrer and a 35 mL stainless steel vial, connected to a thermostat for temperature control, previously purified by washing with a TIBA solution in hexanes, and dried at 50 °C in a stream of propylene. The autoclave was then thermostated at 48 °C. A toluene solution containing the catalyst/cocatalyst mixture was injected in the autoclave by means of nitrogen pressure through the stainless steel vial, the temperature rapidly raised to 50 °C, and the polymerization carried out at constant temperature for 1 h. After venting the unreacted monomer and cooling the reactor to room temperature, the polymer was dried under reduced pressure at 60 °C. The *i*-PP samples were purposely not treated with acidic methanol to avoid isomerization of the vinylidene end groups.

Polymerizations of Ethylene. A 90 mL sample of hexane was introduced at room temperature in a 200 mL glass autoclave, previously purified and purged with ethylene at 35 °C and equipped with magnetic stirrer, temperature indicator, and feeding line for the ethylene. The catalytic system was prepared separately in 10 mL of hexane, by introducing a toluene solution obtained by contacting for 5 min under stirring the metallocene and MAO. The solution was then introduced into the autoclave under ethylene flow, the reactor was closed, and the temperature was increased to 80 °C and the pressure to 4.6 bar g. The total pressure was kept constant by feeding ethylene. After 10 min, the polymerization was stopped by cooling, degassing the reactor, and introducing 1 mL of methanol. The polymer was washed with acidic methanol, then with methanol, and dried in an oven at 60 °C under vacuum.

X-ray Diffraction Structural Analysis. (a) Collection and Reduction of X-ray Diffraction Data. Suitable crystals of **1**, **2**, and **3** were mounted in air on a glass fiber tip onto a goniometer head. Single-crystal X-ray diffraction data were collected on a Siemens SMART CCD area detector diffractometer for **1** and on an Enraf-Nonius CAD-4 diffractometer for **2** and **3**, using graphite-monochromatized Mo Kα radiation (λ = 0.71073 Å) at room temperature. The structure of **3** has been previously reported by others.[24] The two determinations are in agreement, within the experimental error.

For **1**, unit cell parameters were initially obtained from 37 reflections (5° < θ < 20°) taken from 45 frames collected in three different ω regions and eventually refined against 3611 reflections; while for **2** and **3** the setting angles of 25 randomly distributed intense reflections with 10° < θ < 14° were processed by least-squares fitting.

For **1**, more than one hemisphere of reciprocal space was scanned by 0.3° ω steps, collecting 1270 frames each at 40 s exposure. The detector was kept at 5.50(2) cm from the sample. Intensity decay was monitored by re-collecting the initial 50 frames at the end of data collection and analyzing the duplicate reflections. The collected frames were processed for integration; an empirical absorption correction was made on the basis of 3665 symmetry-equivalent reflection intensities (average redundancy: 2.59).[20]

For **2** and **3** data collection was performed by the ω scan method with variable scan speed (maximum time per reflection 75 and 60 s for **2** and **3**, respectively) and variable scan range (1.00 + 0.35 tan θ°). Crystal stability under diffraction was checked by monitoring three standard reflections every 180

(20) Sheldrick, G. M. *Sadabs: program for empirical absorption correction*; University of Göttingen: Göttingen, 1996.
(21) North, A. C. T.; Phillips, D. C.; Mathews, F. S. *Acta Crystallogr., Sect. A* **1968**, *24*, 351.
(22) Altomare, A.; Cascarano, G.; Giacovazzo, C.; Guagliardi, A.; Burla, M. C.; Polidori, G.; Camalli, M. *J. Appl. Crystallogr.* **1994**, *27*, 435.
(23) Sheldrick, G. M. *SHELX97: program for crystal structure refinement*; University of Göttingen: Göttingen, 1997.
(24) Voskoboynikov, A. Z.; Agarkov, A. Yu.; Chernyshev, E. A.; Beletskaya, I. P.; Churakov, A. V.; Kuz'mina, L. G. *J. Organomet. Chem.* **1997**, *530*, 75.

min. An emprical absorption correction was applied using ψ scans of three suitable reflections having χ values close to 90°.[21] The measured intensities were corrected for Lorentz, polarization, and background effects and reduced to F_o^2. Crystal data and data collection parameters are summarized in Table 6.

(b) Structure Solution and Refinement. The structures were solved by direct methods[22] and subsequent Fourier synthesis; they were refined by full-matrix least-squares on F^2 (SHELX97)[23] using all reflections for **1**, and reflections with $I > 2\sigma(I)$ for **2** and **3**. Scattering factors for neutral atoms and anomalous dispersion corrections were taken from the internal library of SHELX97. Weights were assigned to individual observations according to the formula $w = 1/[\sigma^2(F_o^2) + (aP)^2 + bP]$, where $P = (F_o^2 + 2F_c^2)/3$; a and b were chosen to give a flat analysis of variance in terms of F_o^2. Anisotropic displacement parameters were assigned to all non-hydrogen atoms. Hydrogen atoms were placed in idealized position ($d_{C-H} = 0.93$, 0.96, and 0.97 Å for aromatic, methylene, and methyl hydrogen atoms, respectively) and refined riding on their parent atom with an isotropic displacement parameter 1.2 times that of the pertinent carbon atom. The final difference electron density map showed no features of chemical significance, with the largest peaks lying close to the metal atoms. Final conventional agreement indexes and other structure refinement parameters are listed in Table 6.

Acknowledgment. We thank I. E. Nifant'ev for many useful discussions, S. Tartarini and F. Pazzi for the polymerization experiments, and I. Camurati, M. Colonnesi, H. Rychlicki, and F. Piemontesi for NMR analysis of the zirconocenes and the polymers.

Supporting Information Available: Tables of X-ray diffraction data, final atomic coordinates, and full bond distances and angles for **1**−**3**. This material is available free of charge via the Internet at http://pubs.acs.org.

OM990211G